FORCE-MOMENT CAPABILITIES OF REDUNDANTLY-ACTUATED SPATIAL PARALLEL MANIPULATORS USING TWO METHODS

Venus Garg[1], Scott B. Nokleby[2], Juan A. Carretero[3]

[1] *University of New Brunswick, Dept. of Mechanical Engineering, Venus.Garg@unb.ca*

[2] *University of Ontario Institute of Technology, Faculty of Engineering and Applied Science, Scott.Nokleby@uoit.ca*

[3] *University of New Brunswick, Dept. of Mechanical Engineering, Juan.Carretero@unb.ca*

Abstract

From a design perspective, it is important to find the maximum load which can be applied or sustained by a particular parallel manipulator. Force-moment capability analysis is necessary for this purpose. Recently, two methods, namely, a numerical scaling factor method and an analytical explicit method, have been proposed for determining the force-moment capabilities of redundant planar parallel manipulators. In this work, these methods are extended to redundant 6-DOF (degree-of-freedom) spatial manipulators. The methods are applied to the 3-RRRS device. Comparison between the two methods is made. The results show that the explicit method determines higher maximum force-moment capabilities than the scaling factor method. The results for four different cases studied under the explicit method are also presented.

Keywords: spatial parallel manipulator, actuation redundancy, force-moment capabilities, numerical scaling factor method, analytical explicit method, 3-RRRS manipulator.

CAPACITÉS DE FORCE ET MOMENT DES MANIPULATORS PARALLÈLES SPATIAUX REDONDANTS EN UTILISANT DEUX NOUVELLES MÉTHODES

Résumé

D'une perspective de conception, il est important de trouver la charge maximale qui peut être appliquée ou soutenue par un manipulateur parallèle en particulier. L'analyse des capacités de force et moment est nécessaire à cette fin. Récemment, deux nouvelles méthodes d'analyse ont été proposées: une méthode numérique de facteur d'échelle et une méthode explicite analytique. Les deux méthodes ont été proposées pour déterminer les limites de force-moment des manipulateurs parallèles planaires redondants. Dans ce travail, ces deux méthodes sont étendues aux manipulateurs de 6 degrés de liberté spatiaux redondants. Les méthodes sont appliquées au manipulateur 3-RRRS. La comparaison entre les deux méthodes est faite. Les résultats montrent que la méthode explicite détermine des possibilités maximales plus élevées de force-moment que la méthode de facteur d'échelle. Les résultats pour quatre cas différents étudiés sous la méthode explicite sont également présentés.

Mots clés: manipulateur parallèle spatial, redondance d'actionnement, capacité de force-moment, méthode numérique de facteur d'échelle, méthode explicite analytique, manipulateur 3-RRRS.

1 INTRODUCTION

Parallel manipulators (PMs) are closed-loop mechanisms having a fixed base and a moving platform connected by more than one limb. If a manipulator has more actuators than the total degrees-of-freedom (DOF) required for the task, the manipulator is said to be redundant. Redundancy in PMs can be of three types, namely kinematic, actuation, and a combination of both. A kinematically redundant manipulator has more limbs than required to do a particular task. The second type, *i.e.*, actuation redundancy, is the act of increasing the number of actuated joints by actuating one or more of the passive joints without any change to the architecture of the manipulator. Combined redundancy consists of either adding a branch with some of the passive joints actuated or adding extra joints in a branch and making them active. Merlet [1] highlights the importance of redundancy in solving forward displacement problems, obstacle avoidance, kinematic calibration, and improvement in force control.

Actuation redundancy, which will be the focus of this paper, plays a vital role in manipulator applications where completion of the task is critical, such as space applications. Redundant actuation results in removal of actuation singularities (uncontrollable space) and results in a more homogeneous force output as shown by Cheng *et al.* [2]. It also helps in removal of force-degenerate configurations as shown by Firmani and Podhorodeski [3]. If one of the joints fails during operation, actuation redundancy may ensure that the robot is still controllable by using the extra actuated joints and hence, the task can be accomplished. This concept of fault tolerant design and active joint failure, has been studied in detail [4; 5] and it has been shown that actuation redundancy helps in improving fault-tolerance capabilities. Velocity capability analysis of redundantly actuated PMs using velocity ellipsoid has been done [6]. Attempts to optimize parameters like kinematic dexterity and forces at the actuators can be seen in [7]. Other important aspects of actuation redundancy in PMs can be seen in [8-13].

Determination of force-moment capabilities of PMs is a very important factor in designing PMs. Recently, a numerical and an analytical method have been proposed for finding force-moment capabilities of planar parallel manipulators (PPMs). Nokleby *et al.* [14] proposed a methodology for numerically finding the force-moment capabilities of redundantly-actuated PPMs using a 'Scaling Factor Method' which allows actuator limits to be accounted for in the determination of force-moment capabilities. More recently, Zibil *et al.* [15] developed an analytical 'Explicit Method' for resolving the force-moment capabilities of redundantly-actuated PPMs. This explicit method is shown to be more efficient than the scaling factor method for the redundant case. Moreover the explicit method also eliminates the limitations associated with the scaling factor method [15]. Being an analytical method, the explicit method reduces the computational time, allowing for more exhaustive analysis in a shorter time.

In this paper both of the above techniques to determine the force capabilities of PPMs are extended to spatial parallel manipulators. The spatial 3-RRRS, where R refers to a revolute joint and S refers to a spherical joint, shown in Figure 1(a) will be used as an example case. In this work, kinematic analysis of the 3-RRRS is done first using screw theory. Then, the application of the scaling factor method [14] and the recently proposed analytical explicit method [15] to the spatial redundant 3-RRRS is described. Lastly, the two methods are compared and some numerical results are presented.

2 3-RRRS PARALLEL MANIPULATOR

The 3-RRRS manipulator (see Figure 1(a)) under consideration consists of three RRRS branches connecting the fixed base to the moving platform. Each branch, referred to as a limb of the manipulator, has a series of links containing joints. Each limb of the 3-RRRS has a revolute joint at the base followed by a second revolute joint whose axis is perpendicular to the first and a third revolute joint whose axis is parallel to the axis of the second joint. The branch is connected to the moving platform by a spherical joint which can be

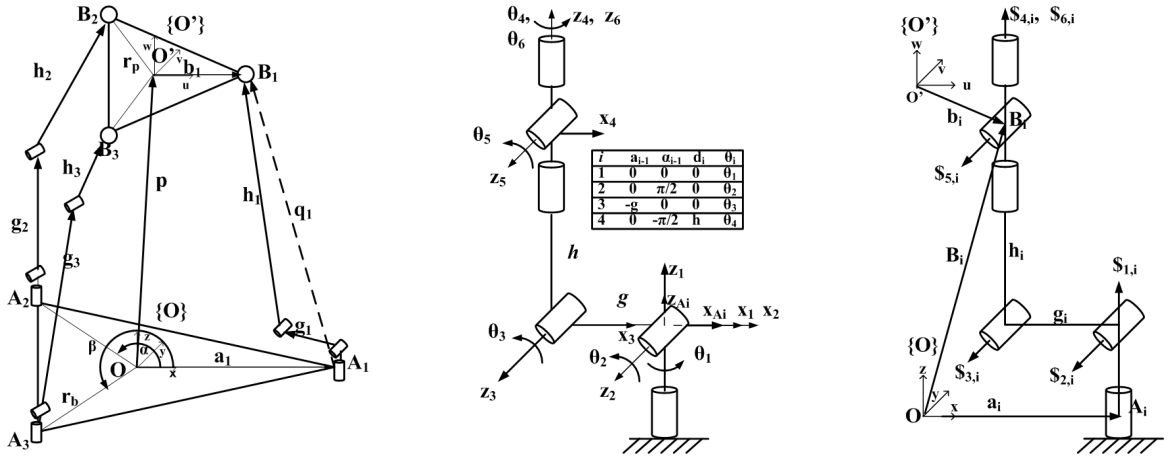

i	a_{i-1}	α_{i-1}	d_i	θ_i
1	0	0	0	θ_1
2	0	$\pi/2$	0	θ_2
3	-g	0	0	θ_3
4	0	$-\pi/2$	h	θ_4

(a) Vector diagram. (b) D&H parameters. (c) Screws for one limb.

Figure 1: Spatial 3RRRS manipulator.

modelled as three consecutive intersecting revolute joints. Thus, as can be demonstrated by the Grübler-Kutsbach mobility criterion [16], the overall mechanism has 6 DOF. All calculations are done in the base frame O which, as seen in Figure 1(a), is the frame located at the centre of the fixed base formed by triangle $\triangle A_1A_2A_3$ and its x and y axes are coplanar with the base's triangle and the x axis points in the direction of point A_1 at the intersection of joints one and two.

In what follows, the actuated joints will be denoted by an underline (*e.g.*, 3-<u>RR</u>RS will mean the first two revolute joints are actuated, whereas, the rest are passive). The redundant case with nine actuated joints, *i.e.*, 3-<u>RRR</u>S is the one considered in this work for the force-moment analysis. The Denavit and Hartenberg (D&H) parameters (see Figure 1(b)) given by Craig [17] are used for solving the forward displacement problem of the 3-<u>RRR</u>S manipulator, from which the inverse displacement problem is then calculated.

For the purpose of analysis, two Cartesian coordinate systems $O(x, y, z)$ and $O^{'}(u, v, w)$ are attached to the fixed base and moving platform, respectively (see Figure 1(a)). The following assumptions are made: points A_1, A_2 and A_3 lie on the $x - y$ plane and B_1, B_2 and B_3 lie on the $u - v$ plane. The origin of the fixed coordinate system is located at the centroid of $\triangle A_1A_2A_3$ and the axis x points along the direction of OA_1. Similarly, the origin $O^{'}$ of the moving coordinate system is located at the centroid of $\triangle B_1B_2B_3$ and the axis u points along the direction of OB_1. For the purpose of analysis, the base and the moving platforms are considered as equilateral triangles with $r_b = 7$ m and $r_p = 6$ m. For simplicity, the orientation of the moving platform is kept the same as the moving platform *i.e.*, frame O and $O^{'}$ are oriented in the same way. The link lengths are taken to be $g = 6$ m and $h = 7$ m, respectively, for the first and second link of all limbs. For the force analysis, the maximum torque of all the actuated joint is set to ± 1 Nm.

3 SCREWS FOR THE 3-RRRS

The force solution can be obtained using screw theory [18]. The screws for one limb are shown in Figure 1(c). Let $\mathbf{s}_{j,i}$ be a unit vector along the jth joint axis of the ith limb. Here, i = 1 to 3 represents the number of limbs and j = 1 to 6 represents the number of joints in each limb. Then the three joint screws representing the manipulator's actuated joints written in the base frame are:

$$ {}^{O}\$_{1,i} = \begin{bmatrix} \mathbf{s}_{1,i} \\ \mathbf{a}_i \times \mathbf{s}_{1,i} \end{bmatrix} \quad {}^{O}\$_{2,i} = \begin{bmatrix} \mathbf{s}_{2,i} \\ \mathbf{a}_i \times \mathbf{s}_{2,i} \end{bmatrix} \quad {}^{O}\$_{3,i} = \begin{bmatrix} \mathbf{s}_{3,i} \\ (\mathbf{B}_i - \mathbf{h}_i) \times \mathbf{s}_{3,i} \end{bmatrix} \tag{1} $$

where $i = 1$ to 3 and $\mathbf{B}_i$ denotes the position vector of the spherical joint expressed in the base frame. The direction vectors $\mathbf{s}_{j,i}$ for the three limbs of the 3-RRRS, which will be used to find the force solution, are:

$$\mathbf{s}_{1,1} = [0,0,1]^T, \quad \mathbf{s}_{2,1} = \mathbf{R}z_{\theta_{1,1}}\,[0,-1,0]^T, \quad \mathbf{s}_{3,1} = \mathbf{s}_{2,1} \tag{2}$$

$$\mathbf{s}_{1,2} = [0,0,1]^T, \quad \mathbf{s}_{2,2} = \mathbf{R}z_{\theta_{1,2}}\,[0,-1,0]^T, \quad \mathbf{s}_{3,2} = \mathbf{s}_{2,2} \tag{3}$$

$$\mathbf{s}_{1,3} = [0,0,1]^T, \quad \mathbf{s}_{2,3} = \mathbf{R}z_{\theta_{1,3}}\,[0,-1,0]^T, \quad \mathbf{s}_{3,3} = \mathbf{s}_{2,3} \tag{4}$$

where $\mathbf{R}z_{\theta_{1,i}}$ is the matrix representing the rotation around the z-axis by angle $\theta_{1,i}$ and vector $\mathbf{h}_i$ is given by:

$$\mathbf{h}_i = \begin{bmatrix} -hc_{\theta_{1,i}}s_{(\theta_{2,i}+\theta_{3,i})} \\ -hs_{\theta_{1,i}}s_{(\theta_{2,i}+\theta_{3,i})} \\ hc_{(\theta_{2,i}+\theta_{3,i})} \end{bmatrix} \tag{5}$$

where $c_{(i)}$ and $s_{(i)}$ denote $\cos\theta_i$ and $\sin\theta_i$, respectively.

A screw reciprocal to all joints except the first actuated joint is a zero-pitch screw intersecting the axes of joints 2 and 3 and passing through the centre of the spherical joint is given by:

$${}^{O}\$_{r1,i} = \begin{bmatrix} \mathbf{s}_{3,i} \\ \mathbf{B}_i \times \mathbf{s}_{3,i} \end{bmatrix} \tag{6}$$

Similarly, the associated reciprocal screw to the second actuated joint is given by:

$${}^{O}\$_{r2,i} = \begin{bmatrix} \hat{\mathbf{h}}_i \\ \mathbf{B}_i \times \hat{\mathbf{h}}_i \end{bmatrix} \tag{7}$$

Finally, a screw reciprocal to all joints expect the third is given by:

$${}^{O}\$_{r3,i} = \begin{bmatrix} (\hat{\mathbf{h}}_i + \hat{\mathbf{g}}_i)/|(\hat{\mathbf{h}}_i + \hat{\mathbf{g}}_i)| \\ \mathbf{B}_i \times (\hat{\mathbf{h}}_i + \hat{\mathbf{g}}_i)/|(\hat{\mathbf{h}}_i + \hat{\mathbf{g}}_i)|. \end{bmatrix} \tag{8}$$

Vector $\mathbf{g}_i$ is given by:

$$\mathbf{g}_i = \begin{bmatrix} -gc_{\theta_{1,i}}c_{\theta_{2,i}} \\ -gs_{\theta_{1,i}}c_{\theta_{2,i}} \\ -gs_{\theta_{2,i}} \end{bmatrix} \tag{9}$$

and $\hat{\mathbf{h}}_i$ and $\hat{\mathbf{g}}_i$ represent unit vectors in the direction of $\mathbf{h}_i$, and $\mathbf{g}_i$, respectively.

Now, from the 3-RRRS's reciprocal screws obtained in equations (6) to (8), the following equations can be obtained:

$$\$_{rj,i} \circledast \$_{j,i} = 0, \text{ for } j \neq i, \quad i,j = 1 \text{ to } 3 \tag{10}$$

where $\circledast$ denotes a reciprocal product.

Considering each limb as an open-loop chain, the instantaneous twist of the moving platform in terms of the joint screws is given by:

$$\$_P = \dot{\theta}_{1,i}\$_{1,i} + \dot{\theta}_{2,i}\$_{2,i} + \dot{\theta}_{3,i}\$_{3,i} + \dot{\theta}_{4,i}\$_{4,i} + \dot{\theta}_{5,i}\$_{5,i} + \dot{\theta}_{6,i}\$_{6,i} \tag{11}$$

Taking the reciprocal product of both sides of equation (11) with the reciprocal screws $\$_{rj,i}$, the following equations are obtained:

$$\$_{rj,i} \circledast \$_P = \$_{rj,i} \circledast \$_{j,i}\dot{\theta}_{1,i} \tag{12}$$

Now, a matrix $[\$']$, called the associated reciprocal screw (ARS) matrix is defined as:

$$[\$'] = [\$_{rj,i}] \tag{13}$$

Next, the matrix $\mathbf{D}$, called the diagonal matrix of the inverses of the reciprocal products of the actuated joints and their associated reciprocal screws, is defined as:

$$\mathbf{D} = diag\left[\frac{1}{\$_{rj,i} \circledast \$_{j,i}}\right] \tag{14}$$

Let $w_{j,i}$ be the wrench intensity of the jth actuated joint in branch i. If a manipulator has m branches and n_i is the number of actuated joints in the ith branch, then the relation between the wrench intensity and the torque in terms of the reciprocal screw quantities is given as:

$$w_{j,i} = \frac{\tau_{j,i}}{\$_{rj,i} \circledast \$_{j,i}} \quad \textit{i.e.,} \tag{15}$$

$$\mathbf{w} = \mathbf{D}\boldsymbol{\tau} \tag{16}$$

and the force applied by the end effector is given as:

$$\mathbf{F} = \sum_{i=1}^{m}\left(\sum_{j=1}^{n_i} \$_{rj,i} w_{j,i}\right) \quad \textit{i.e.,} \tag{17}$$

$$\mathbf{F} = [\$']\mathbf{w} \tag{18}$$

Therefore, using matrices $[\$']$ and $\mathbf{D}$, the forward and inverse force (IF) solution can be derived as:

$$\mathbf{F} = ([\$']\mathbf{D})\boldsymbol{\tau} \tag{19}$$

$$\boldsymbol{\tau} = ([\$']\mathbf{D})^{-1}\mathbf{F} \tag{20}$$

4 SCALING FACTOR METHOD

The scaling factor method [14] is a numerical force-moment computational method that allows the actuator limits to be easily incorporated into the problem of determining force-moment capabilities of PMs. The method is explained in this section. A unit wrench $\$_F$ will be used to represent the desired wrench direction:

$$\mathbf{F}_{app} = f_{app}\$_F \tag{21}$$

where f_{app} is the wrench intensity of $\mathbf{F}_{app}$. To generate a force capability plot using the IF solution, one needs to find the maximum wrench intensity, f_{app}, in order to maximize the magnitude of $\mathbf{F}_{app}$, while still remaining within the torque/force limits of the actuated joints.

For the redundantly actuated case, $[[\$']\mathbf{D}]$ forms a non-square matrix. So, the right Moore-Penrose pseudo-inverse[1] is used to find its inverse. Out of the infinite possible solutions, the Moore-Penrose solution corresponds to the particular solution with a minimum 2-norm. Therefore, the inversion of $[[\$']\mathbf{D}]$ yields:

$$\boldsymbol{\tau}_{\$_F} = \left[[\$']\mathbf{D}\right]^{+}\$_F \tag{22}$$

[1]Right Moore Penrose pseudo-inverse of a matrix $\mathbf{Q}$ is: $[\mathbf{Q}]^{+} = \mathbf{Q}^T(\mathbf{Q}\mathbf{Q}^T)^{-1}$

where $\boldsymbol{\tau}_{\$_F}$ is the vector of torques/forces to create the unit wrench $\$_F$ in the direction of the desired $\mathbf{F}_{app}$. Note, the screws are expressed in terms of the base frame $\{O\}$, and the force also has to be expressed in the base frame to do all the torque and scaling factor calculations. Since all the maximum actuated joint torque and force limits, $\tau_{j,i_{max}}$ are known for all actuated joints j of each branch i, scaling factors for each actuated joint can be found using:

$$\gamma_{j,i} = \left| \frac{\tau_{j,i_{max}}}{\tau_{\$_F j,i}} \right| \tag{23}$$

where $\gamma_{j,i}$ is the scaling factor and $\tau_{\$_{F_{j,i}}}$ is the torque/force of the jth actuated joint of the ith branch for a unit wrench $\$_F$ in the desired force direction. The scaling factors of equation (23) can be placed in a set. The scaling factor (Υ) is the maximum factor which all joint torques/forces can be scaled by and still remain at or below their corresponding maximum values. It is given by the minimum of the scaling factors $\gamma_{j,i}$ as:

$$\Upsilon = \min(\gamma_{j,i}) \tag{24}$$

Therefore, the maximum wrench, $\mathbf{F}_{app}$, that can be applied in the direction $\$_F$ is:

$$\mathbf{F}_{app} = \Upsilon \left[[\$^{'}]\mathbf{D} \right] \boldsymbol{\tau}_{\$_F} \tag{25}$$

To create a force capability plot using the inverse force solution, $\$_F$ is varied as a set of 974 directions evenly distributed on a sphere. This method is useful in application since often the direction of the applied force is known and the knowledge of the magnitude of the load is desired. The maximum possible load magnitude is the quantity that is directly obtained from the above minimum scaling factor based IF solution.

5 EXPLICIT METHOD

Zibil *et al.* [15] recently proposed a explicit method for determining the force-moment capabilities of redundantly actuated PPMs. The method determines the maximum number of actuators that can be set to their maximum limits thereby maximizing the wrench to be applied/sustained. This explicit method, is extended here to the spatial case.

5.1 Planar Case [15]

In general, if a manipulator has k actuated joints and n is the dimension of the space which it can span ($n \leq 6$), then, the forward force solution can be written as:

$$\left[[\$^{'}]\mathbf{D} \right]_{n \times k} \boldsymbol{\tau}_{k \times 1} = \mathbf{F}_{n \times 1} \tag{26}$$

For the planar 3-RRR $n = 3$, therefore, $\mathbf{F}$ can be defined as $[f \cos\alpha \;\; f \sin\alpha \;\; m_z]$. The matrix $[[\$^{'}]\mathbf{D}]$ is known as it depends only on the structural parameters and position and orientation of the end effector which is known. Therefore, there are $k + 3$ unknowns (k elements of τ and 3 elements of $\mathbf{F}$). Equation (26), for $n = 3$, represents three equations so it can be used to determine three of these unknowns and the remaining k unknowns can be set arbitrarily. The basic idea is to set the number of unknowns to the maximum value so as to maximize the applied/suatained wrench. Four cases were considered in [15] for the 3-RRR. 1) Maximum force with a prescribed moment, 2) Maximum applicable force with an associated moment, 3) Maximum moment with a prescribed force, and 4) Maximum applicable moment with an associated force. The first case is briefly explained here.

In the first case, α and m_z are specified, therefore, there are $k - 2$ unknowns. In other words, $k - 2$ torques can be set to their maximum quantities (τ_{max}). Equation (26) is rearranged to find the two torques in transition and the wrench intensity f. The formulations of all four cases can be found in [15].

5.2 Spatial Case

For the spatial 3-RRRS, $n = 6$, therefore equation (26) becomes:

$$\Big[[\$^{'}]\mathbf{D}\Big]_{6\times k}\ \boldsymbol{\tau}_{k\times 1} = \mathbf{F}_{6\times 1} \tag{27}$$

where $\mathbf{F}$ can be defined as $[f\cos\alpha \quad f\cos\beta \quad f\sin\gamma \quad m_x \quad m_y \quad m_z]$. The matrix $[[\$^{'}]\mathbf{D}]$ is known as it depends only on the structural parameters and position and orientation of the end effector which are known. Therefore, there are $k\ +\ 6$ unknowns (k elements of τ and 6 elements of $\mathbf{F}$). Equation (27) represents six equations so it can be used to determine six of these unknowns and the remaining k unknowns can be set arbitrarily. The four cases considered for PPMs, now applied to spatial PMs are explained in the following subsections.

5.2.1 Maximum force with a prescribed moment (Case 1)

In this case, direction angles[2] α, β and moments m_x, m_y, m_z are specified (prescribed), therefore, $k-5$ variables can be defined arbitrarily, *i.e.*, $k-5$ actuator torques can be set to their maximum quantities (τ_{max}). For the 3-RRRS, $k = 9$, therefore, there are four maxed-out actuators, and equation (27) can be rearranged to find the five torques in transition and the force magnitude f as:

$$\begin{bmatrix} -\$^{'}D_{1,t1} & ... & -\$^{'}D_{1,t5} & \cos\alpha \\ -\$^{'}D_{2,t1} & ... & -\$^{'}D_{2,t5} & \cos\beta \\ -\$^{'}D_{3,t1} & ... & -\$^{'}D_{3,t5} & \cos\gamma \\ -\$^{'}D_{4,t1} & ... & -\$^{'}D_{4,t5} & 0 \\ -\$^{'}D_{5,t1} & ... & -\$^{'}D_{5,t5} & 0 \\ -\$^{'}D_{6,t1} & ... & -\$^{'}D_{6,t5} & 0 \end{bmatrix} \begin{bmatrix} \tau_{t1} \\ \tau_{t2} \\ \tau_{t3} \\ \tau_{t4} \\ \tau_{t5} \\ f \end{bmatrix} = \begin{bmatrix} \$^{'}D_{1,m1} & \$^{'}D_{1,m2} & ... & \$^{'}D_{1,m4} \\ \$^{'}D_{2,m1} & \$^{'}D_{2,m2} & ... & \$^{'}D_{2,m4} \\ \$^{'}D_{3,m1} & \$^{'}D_{3,m2} & ... & \$^{'}D_{3,m4} \\ \$^{'}D_{4,m1} & \$^{'}D_{4,m2} & ... & \$^{'}D_{4,m4} \\ \$^{'}D_{5,m1} & \$^{'}D_{5,m2} & ... & \$^{'}D_{5,m4} \\ \$^{'}D_{6,m1} & \$^{'}D_{6,m2} & ... & \$^{'}D_{6,m4} \end{bmatrix} \begin{bmatrix} \pm\tau_{m1} \\ \pm\tau_{m2} \\ \pm\tau_{m3} \\ \pm\tau_{m4} \end{bmatrix} - \begin{bmatrix} 0 \\ 0 \\ 0 \\ m_x \\ m_y \\ m_z \end{bmatrix} \tag{28}$$

where $\$^{'}D_{i,tj}$ and $\$^{'}D_{i,mj}$ are the elements of the $[\$^{'}\mathbf{D}]$ matrix corresponding to the transition and maxed-out actuator indices, respectively. Equation (28) can then be solved to find the force magnitude f. The sign of the actuator value must again be taken into account while choosing the $k-5$ actuators from k actuators. The number of combinations of actuators n_C is given by:

$$n_C = n_A\ \times\ n_S = \frac{k!}{(k-(k-5))!\times(k-5)!}\ \times\ 2^{k-5} = 2016 \tag{29}$$

where n_A refers to $k-5$ actuators chosen from k actuators and n_S refers to the sign combinations of these $k-5$ actuators. Equation (28) is solved for all n_C possible maxed-out combinations for the first wrench direction. The combination which yields the solution with no joint torque exceeding the limits and the maximum force magnitude is selected as the solution for the first direction.

The next direction is picked close to the proceeding one where the maximum force magnitude is solved using the same combination of maxed-out torques as this saves a lot of computational time. The same process is repeated for contiguous directions until one of the torques in transition exceeds the maximum limit. When this happens, equation (28) is solved again for all n_C actuator combinations and the combination which yields the solution with maximum force is selected as the solution for the current direction. The process is repeated until the solutions for all directions are obtained. Therefore, the max-max and min-max of the maximum sustainable force can be obtained. The max-max (maximum of the maximum forces) gives

[2]Only two angles out of three need to be specified as the third is given by $\cos^2\alpha + \cos^2\beta + \cos^2\gamma = 1$, as the directions are varied in terms of a homogeneous unit sphere.

the maximum applicable/sustainable force in a particular direction for a given pose whereas the min-max (minimum of the maximum forces) corresponds to the force which the manipulator can apply/sustain in any direction for a given pose. In other words, the min-max is the minimum force which the manipulator can sustain in all directions for a particular position and orientation of the end effector. It is the min-max force that is important when designing any PM as it is the one determining its minimum capabilities.

5.2.2 Maximum applicable force with an associated moment (Case 2)

In this case, the moment is considered as an unknown variable as the maximum force will have some associated moment. That is why the maximum magnitude of force found in this case is called maximum applicable force as compared to just maximum force for Case 1, as it has an associated moment component along with it which cannot be fixed by the user. There are $(k-5+3$ (unknown moment)$) = k-2$ actuator torques that are maxed-out and two torques are in transition for the 3-RRRS ($k = 9$). The number of maxed-out actuator combinations is given by:

$$n_C = n_A \times n_S = \frac{k!}{(k-(k-2))! \times (k-2)!} \times 2^{k-2} = 4608 \tag{30}$$

and the matrix formulation for this case is:

$$\begin{bmatrix} -\$^{'}D_{1,t1} & -\$^{'}D_{1,t2} & \cos\alpha & 0 & 0 & 0 \\ -\$^{'}D_{2,t1} & -\$^{'}D_{2,t2} & \cos\beta & 0 & 0 & 0 \\ -\$^{'}D_{3,t1} & -\$^{'}D_{3,t2} & \cos\gamma & 0 & 0 & 0 \\ -\$^{'}D_{4,t1} & -\$^{'}D_{4,t2} & 0 & 1 & 0 & 0 \\ -\$^{'}D_{5,t1} & -\$^{'}D_{5,t2} & 0 & 0 & 1 & 0 \\ -\$^{'}D_{6,t1} & -\$^{'}D_{6,t2} & 0 & 0 & 0 & 1 \end{bmatrix} \begin{bmatrix} \tau_{t1} \\ \tau_{t2} \\ f \\ m_x \\ m_y \\ m_z \end{bmatrix} = \begin{bmatrix} \$^{'}D_{1,m1} & \$^{'}D_{1,m2} & \dots & \$^{'}D_{1,m7} \\ \$^{'}D_{2,m1} & \$^{'}D_{2,m2} & \dots & \$^{'}D_{2,m7} \\ \$^{'}D_{3,m1} & \$^{'}D_{3,m2} & \dots & \$^{'}D_{3,m7} \\ \$^{'}D_{4,m1} & \$^{'}D_{4,m2} & \dots & \$^{'}D_{4,m7} \\ \$^{'}D_{5,m1} & \$^{'}D_{5,m2} & \dots & \$^{'}D_{5,m7} \\ \$^{'}D_{6,m1} & \$^{'}D_{6,m2} & \dots & \$^{'}D_{6,m7} \end{bmatrix} \begin{bmatrix} \pm\tau_{m1} \\ \pm\tau_{m2} \\ \pm\tau_{m3} \\ \pm\tau_{m4} \\ \pm\tau_{m5} \\ \pm\tau_{m6} \\ \pm\tau_{m7} \end{bmatrix} \tag{31}$$

As before, the maxed-out actuator combinations that return solutions where at least one of the actuator torques in transition exceed their corresponding maximum values are not taken into account. From the remaining solutions, the one yielding the highest force magnitude is selected as the solution for the first direction. The maxed-out actuator signs corresponding to the solution for the first direction are kept the same for contiguous directions. The next directions are then solved using the same actuator combination as the previous one until one of the torques in transition exceeds its maximum value. When this happens, equation (31) is solved again for all n_C actuator combinations for the maximum force condition.

5.2.3 Maximum moment with a prescribed force (Case 3)

This case is similar to Case 1 for the spatial case and $k-5$, *i.e.*, four actuators can be maxed-out. The direction of the moment is now varied and force (f_x, f_y, f_z) is fixed. The matrix formulation is:

$$\begin{bmatrix} -\$^{'}D_{1,t1} & \dots & -\$^{'}D_{1,t5} & 0 \\ -\$^{'}D_{2,t1} & \dots & -\$^{'}D_{2,t5} & 0 \\ -\$^{'}D_{3,t1} & \dots & -\$^{'}D_{3,t5} & 0 \\ -\$^{'}D_{4,t1} & \dots & -\$^{'}D_{4,t5} & \cos\alpha \\ -\$^{'}D_{5,t1} & \dots & -\$^{'}D_{5,t5} & \cos\beta \\ -\$^{'}D_{6,t1} & \dots & -\$^{'}D_{6,t5} & \cos\gamma \end{bmatrix} \begin{bmatrix} \tau_{t1} \\ \tau_{t2} \\ \tau_{t3} \\ \tau_{t4} \\ \tau_{t5} \\ m \end{bmatrix} = \begin{bmatrix} \$^{'}D_{1,m1} & \dots & \$^{'}D_{1,m4} \\ \$^{'}D_{2,m1} & \dots & \$^{'}D_{2,m4} \\ \$^{'}D_{3,m1} & \dots & \$^{'}D_{3,m4} \\ \$^{'}D_{4,m1} & \dots & \$^{'}D_{4,m4} \\ \$^{'}D_{5,m1} & \dots & \$^{'}D_{5,m4} \\ \$^{'}D_{6,m1} & \dots & \$^{'}D_{6,m4} \end{bmatrix} \begin{bmatrix} \pm\tau_{m1} \\ \pm\tau_{m2} \\ \pm\tau_{m3} \\ \pm\tau_{m4} \end{bmatrix} - \begin{bmatrix} f_x \\ f_y \\ f_z \\ 0 \\ 0 \\ 0 \end{bmatrix} \tag{32}$$

Equation (32) is solved for all 2016 combinations for this case. The combination which yields the maximum magnitude of moment m is selected as the solution for the first direction. Again, to save computational time, the next directions are solved in the same manner as mentioned in the previous cases, the only difference is instead of the maximum magnitude of the force, the maximum magnitude of the moment is the condition being checked.

5.2.4 Maximum applicable moment with an associated force (Case 4)

This case is similar to Case 2 described before, for which, $k-2$ actuators can be set to their maximum capabilities ($n_C = 4608$). Equation (27) is rearranged to solve for the moment magnitude and associated force values:

$$\begin{bmatrix} -\$'D_{1,t1} & -\$'D_{1,t2} & 0 & 1 & 0 & 0 \\ -\$'D_{2,t1} & -\$'D_{2,t2} & 0 & 0 & 1 & 0 \\ -\$'D_{3,t1} & -\$'D_{3,t2} & 0 & 0 & 0 & 1 \\ -\$'D_{4,t1} & -\$'D_{4,t2} & \cos\alpha & 0 & 0 & 0 \\ -\$'D_{5,t1} & -\$'D_{5,t2} & \cos\beta & 0 & 0 & 0 \\ -\$'D_{6,t1} & -\$'D_{6,t2} & \cos\gamma & 0 & 0 & 0 \end{bmatrix} \begin{bmatrix} \tau_{t1} \\ \tau_{t2} \\ m \\ f_x \\ f_y \\ f_z \end{bmatrix} = \begin{bmatrix} \$'D_{1,m1} & \$'D_{1,m2} & ... & \$'D_{1,m7} \\ \$'D_{2,m1} & \$'D_{2,m2} & ... & \$'D_{2,m7} \\ \$'D_{3,m1} & \$'D_{3,m2} & ... & \$'D_{3,m7} \\ \$'D_{4,m1} & \$'D_{4,m2} & ... & \$'D_{4,m7} \\ \$'D_{5,m1} & \$'D_{5,m2} & ... & \$'D_{5,m7} \\ \$'D_{6,m1} & \$'D_{6,m2} & ... & \$'D_{6,m7} \end{bmatrix} \begin{bmatrix} \pm\tau_{m1} \\ \pm\tau_{m2} \\ \pm\tau_{m3} \\ \pm\tau_{m4} \\ \pm\tau_{m5} \\ \pm\tau_{m6} \\ \pm\tau_{m7} \end{bmatrix} \tag{33}$$

Using the above equation with the method described earlier, the force-moment capabilities can be found over the entire workspace.

6 RESULTS

The maximum applied force magnitude was calculated using the two methods for the redundant 3-RRRS and the results for various positions of the end effector are tabulated in Table 1. The architectural and torque parameters used for the 3-RRRS are the ones mentioned in Section 2. It is important to note that the comparison is made for the first case of the explicit method with the scaling factor method (using only the right Moore-Penrose pseudo-inverse) as this is the only case of the explicit method which can be compared with the scaling factor method. Note that in this case, the maximum magnitude of the applied/sustainable force is found and the moment values are set to zero for the comparison given in Table 1.

From the results it can be seen that the maximum magnitude of force given by the explicit method is higher than the scaling factor method. This result is due to the fact that a greater number of actuators are performing at their maximum or very close to their maximum limit. In the scaling factor method, only the particular solution is used and not the particular solution plus the homogeneous solution as was done in [14]. The right Moore-Penrose pseudo-inverse was used for the particular solution. Not incorporating the homogeneous solution was another factor that caused the results with the scaling factor method to be lower. The force-capability plots for Case 1 using the explicit method at various positions of the end effector can be seen in Figure 2. The force polyhedra represent the forces the manipulator can apply/sustain in all the applied directions for a particular position of the end effector. Out of these magnitudes, the maximum value is the one taken as the maximum force magnitude that the manipulator can apply/sustain for that particular position and this is the one compared in Table 1.

The force capability plots corresponding to Case 2 of the explicit method can be seen in Figure 3. The maximum magnitudes of forces sustainable/applicable by the manipulator for this case are higher than for Case 1 compared to the same positions of the end effector. This is because in Case 1, four actuators torques are maxed-out and five are in transition while in Case 2 seven actuator torques are maxed-out and only two are in transition, thus leading to a higher sustainable/applicable force. The other results of this case are presented in Table 2 along with the values of the associated moments at the maximum force magnitude.

For the two cases, which involve finding the maximum magnitude of moment, the results are tabulated in Table 3. In Case 3 the prescribed force value is set to 0 N. In general, it can be set to any required value. From the results it can be seen that the moment magnitudes calculated from the case in which the force is associated are higher than the case in which the force is prescribed. This can be understood from the reason that in Case 4, seven actuator torques are set to maximum as compared to four maximum torques corresponding to Case 3.

Table 1: Explicit Method *vs.* Scaling Factor Method

Position	Explicit Method: Case 1	Scaling Factor Method
(x; y; z)	Maximum Force Magnitude (N)	Maximum Force Magnitude (N)
(0; 0; 4)	0.7124	0.5925
(0; 0; 6)	0.7519	0.6362
(0; 0; 8)	0.8513	0.7174
(0; 0; 10)	1.0541	0.8887
(1; 2; 4)	0.9233	0.8574
(1; 2; 8)	0.8100	0.7196
(1; 2; 9)	0.8573	0.7453

Table 2: Explicit Method: Case 2

(x; y; z)	Maximum Force Magnitude (N)	Associated Moment Magnitude (Nm)
(0; 0; 4)	2.5173	12.4770
(0; 0; 6)	2.3660	16.3360
(0; 0; 8)	2.3092	20.1230
(0; 0; 10)	2.3141	23.9280
(1; 2; 4)	1.6210	8.2242
(1; 2; 8)	1.5614	9.6003
(1; 2; 9)	1.5756	11.4540

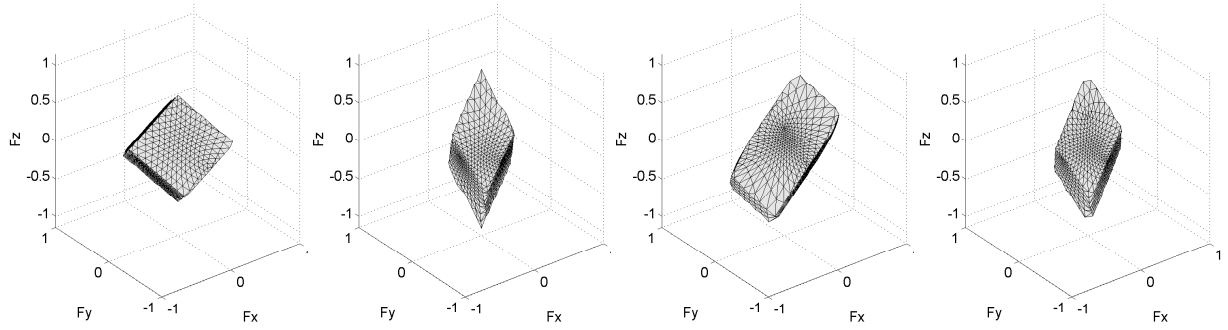

(a) Position (0; 0; 4). (b) Position (0; 0; 10). (c) Position (1; 2; 4). (d) Position (1; 2; 8).

Figure 2: Force plots for the redundant 3-RRRS manipulator for Case 1.

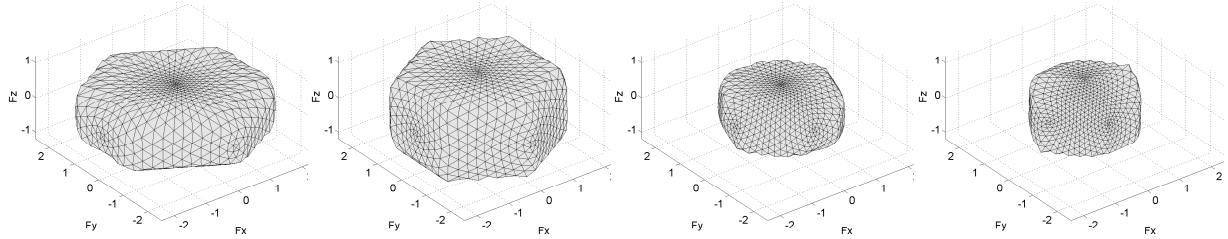

(a) Position (0; 0; 4). (b) Position (0; 0; 10). (c) Position (1; 2; 4). (d) Position (1; 2; 8).

Figure 3: Force plots for the redundant 3-RRRS manipulator for Case 2.

Table 3: Explicit Method: Case 3 and Case 4

Position	Case 3	Case 4
(x; y; z)	Maximum Moment Magnitude (Nm)	Maximum Moment Magnitude (Nm)
(0; 0; 4)	18.0254	18.5187
(0; 0; 6)	18.0264	18.7158
(0; 0; 8)	18.0629	19.3615
(0; 0; 10)	18.1143	23.9029
(1; 2; 4)	6.4565	10.7824
(1; 2; 8)	4.8384	14.5804
(1; 2; 9)	5.0761	15.9612

From the results of all four cases it can be seen that as the number of maxed-out torques which can be explicitly set to the maximum value is changed, the force/moment capability is greatly affected. Also, the more redundant the manipulator is, the greater the number of torques which can be set to their maximum values and the larger the force/moment that the manipulator can sustain/apply. So, actuation redundancy has a vital role in enhancing the force and moment capabilities of PMs. In addition to that, the first and the third case which involve finding the maximum force and maximum moment, are useful in practical applications where the user wants to specifically set the value of moment and force, and then find the maximum value of the force/moment that the manipulator can sustain/apply. These two cases could further help in choosing the design variables for the manipulator depending on the task it is required to do and hence, become a part of the task planning process.

7 CONCLUSION

Two methods, namely a scaling factor method and an explicit method, for finding the force-moment capabilities have been successfully extended to redundant spatial manipulators and compared. The methods are applicable to both non-redundant and redundant spatial PMs. The explicit method, being more efficient, can be incorporated in the design of PMs. Further, this method can be extended to other spatial PMs and the force-moment capability analysis can be done. Also, use of the explicit method in finding the workspace regions where the manipulator can sustain/apply a particular desired value of force/moment is possible.

REFERENCES

[1] J.-P. Merlet. Redundant parallel manipulators. *Lab. Robotics and Automation*, 8(1):17–24, 1996.

[2] H. Cheng, G.F. Liu, Y.K. Yiu, Z.H. Xiong, and Z.X. Li. Advantages and dynamics of parallel manipulators with redundant actuation. In *Proceedings of the 2001 IEEE/RSJ International Conference on Intelligent Robots and Systems*, pages 171 – 176, Maui, USA, October 29 - November 3 2001.

[3] F. Firmani and R. P. Podhorodeski. Force-unconstrained poses for a redundantly-actuated planar parallel manipulator. *Mechanism and Machine Theory*, 39(5):459 – 476, 2004.

[4] M. Hassan and L. Notash. Analysis of active joint failure in parallel robot manipulators. *Journal of Mechanical Design, Transactions of the ASME*, 126(6):959 – 968, 2004.

[5] L. Notash and L. Huang. On the design of fault tolerant parallel manipulators. *Mechanism and Machine Theory*, 38(1):85 – 101, 2003.

[6] S. Krut, O. Company, and F. Pierrot. Velocity performance indices for parallel mechanisms with actuation redundancy. *Robotica*, 22:129 – 39, March 2004.

[7] R. Kurtz and V. Hayward. Multiple-goal kinematic optimization of a parallel spherical mechanism with actuator redundancy. *IEEE Transactions on Robotics and Automation*, 8(5):644 – 651, 1992.

[8] T. Kokkinis and P. Millies. Parallel robot-arm regional structure with actuational redundancy. *Mechanism and Machine Theory*, 26(6):629 – 641, 1991.

[9] P. Buttolo and B. Hannaford. Advantages of actuation redundancy for the design of haptic displays. *ASME, Dynamic Systems and Control Division (Publication) DSC*, 57-2:623 – 630, 1995.

[10] L. Beiner. Redundant actuation of a closed-chain manipulator. *Adv. Robotics*, 11(3):233 – 245, 1997.

[11] S. Kim. Operational quality analysis of parallel manipulators with actuation redundancy. *Proceedings - IEEE International Conference on Robotics and Automation*, 3:2651 – 2656, 1997.

[12] S. Leguay-Durand and C. Reboulet. Optimal design of a redundant spherical parallel manipulator. *Robotica*, 15(4):399 – 405, 1997.

[13] C. Reboulet and S. Durand-Leguay. Optimal design of redundant parallel mechanism for endoscopic surgery. *IEEE International Conference on Intelligent Robots and Systems*, 3:1432 – 1437, 1999.

[14] S.B. Nokleby, R. Fisher, R.P. Podhorodeski, and F. Firmani. Force capabilities of redundantly-actuated parallel manipulators. *Mechanism and Machine Theory*, 40(5):578 – 599, 2005.

[15] A. Zibil, F. Firmani, S.B. Nokleby, and R.P. Podhorodeski (Article in Press). An explicit method for determining the force-moment capabilities of redundantly-actuated planar parallel manipulators. *Transactions of the ASME, Journal of Mechanical Design*.

[16] K. H. Hunt and J.K. Davidson. *Robots and Screw Theory: Applications of Kinematics and Statics to Robotics*. Oxford Science Publications, Oxford, New York, 2004.

[17] J.J. Craig. *Introduction to Robotics: Mechanics and Control - Second Edition*. Addison-Wesley Publishing Company, Don Mills, Ontario, Canada, 1989.

[18] L.-W. Tsai. *Robot Analysis - The Mechanics of Serial and Parralel Manipulators*. Wiley-Interscience, Third Avenue, New York, 1999.